

Supporting Information

Bipolar membrane polarization behavior with systematically varied interfacial areas in the junction region

Subarna Kole^a, Gokul Venugopalan^a, Deepra Bhattacharya^a, Le Zhang^a, John Cheng^a, Bryan Pivovar^b, and Christopher G. Arges^{a}*

^aCain Department of Chemical Engineering, Louisiana State University, Baton Rouge, LA 70803 USA

^bChemical and Materials Science Center, National Renewable Energy Laboratory, Golden, CO 80401 USA

Corresponding author e-mail: carges@lsu.edu

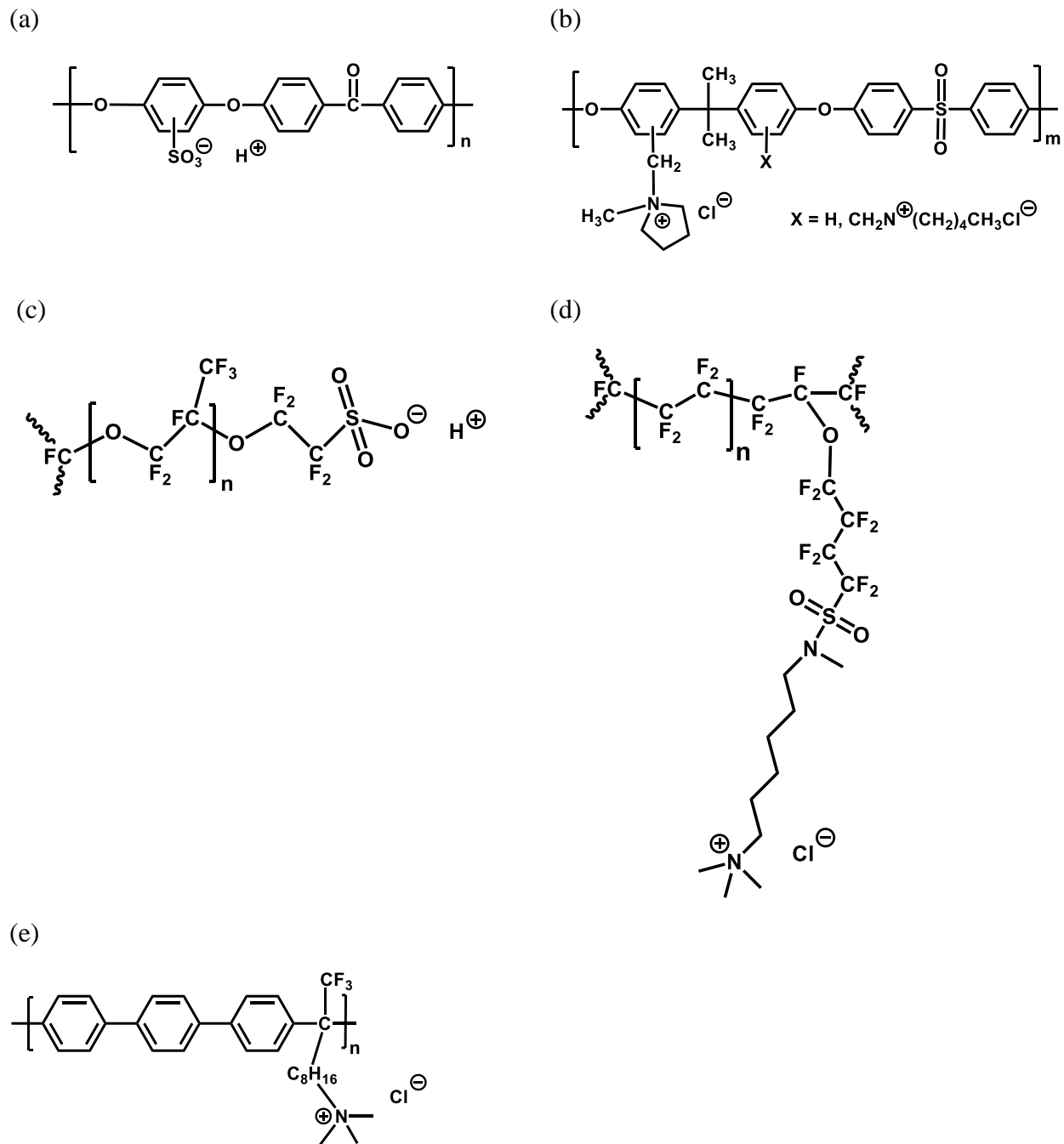
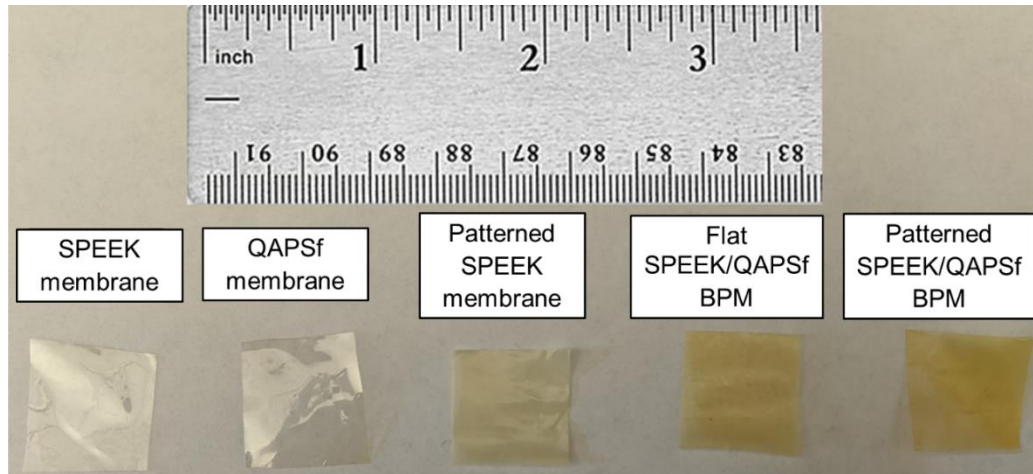


Figure S1. Chemical structures of ionomers used for synthesizing BPMs (a) Sulfonated poly(arylene ether ether ketone) (SPEEK) (b) Quaternary ammonium poly(arylene ether) sulfone (QAPSf) (c) Nafion™ (d) Perfluorinated anion exchange membrane (PF AEM) (e) Orion AEM

(a)



(b)

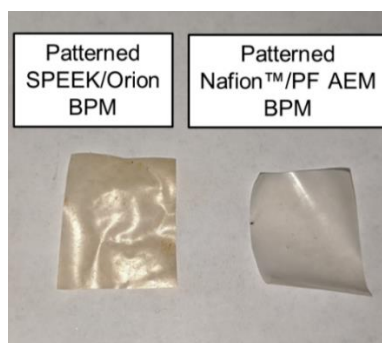
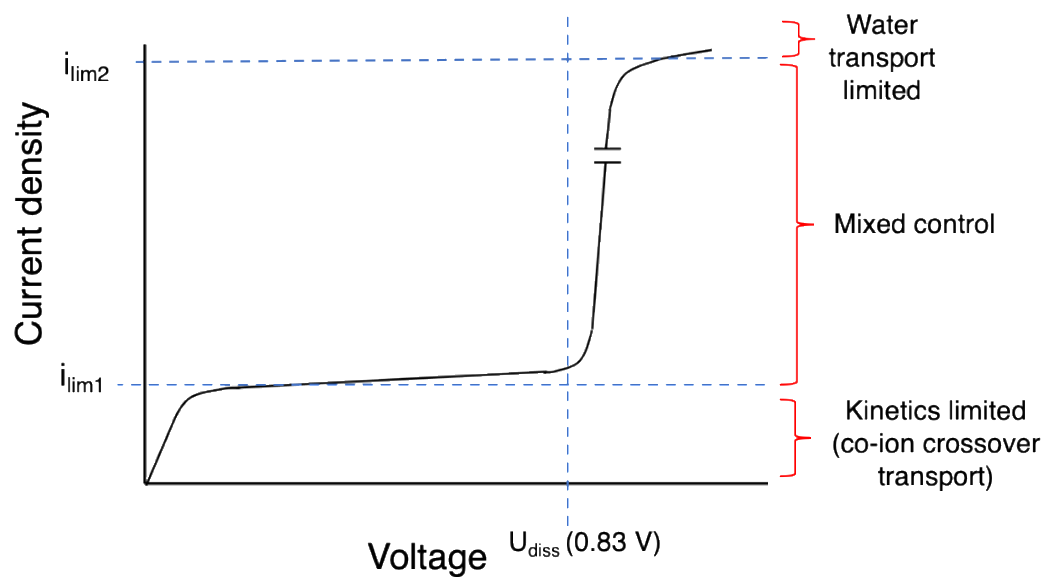


Figure S2. Pictures of (a) flat and patterned SPEEK, QAPSf and BPMs (b) other BPM chemistries fabricated.

Table S1. Thicknesses of various BPMs used in this work

BPM chemistry	Thickness (flat BPM)	Thickness (patterned BPM)
SPEEK/QAPSf BPM	70 μm	74 μm
Nafion™/PF AEM BPM	91 μm	104 μm
SPEEK/Orion AEM BPM	119 μm	124 μm

(a)



(b)

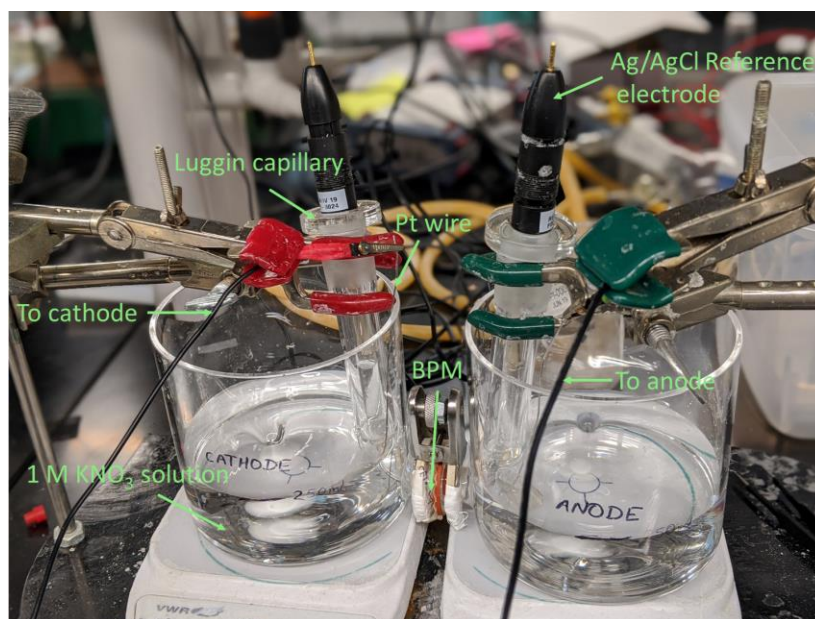


Figure S3. a.) Anticipated polarization behavior of BPMs based upon literature precedent^[1]. The first limiting current arise from co-ion inclusion in the membranes and ionic species crossover. b.) Picture of home-made 4-point cell for polarization experiments.

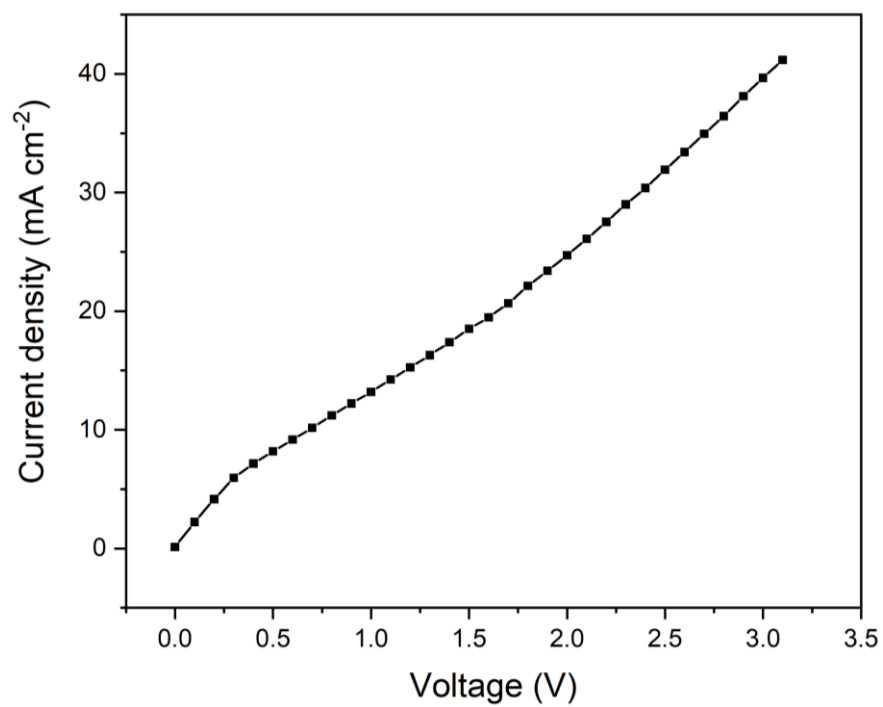
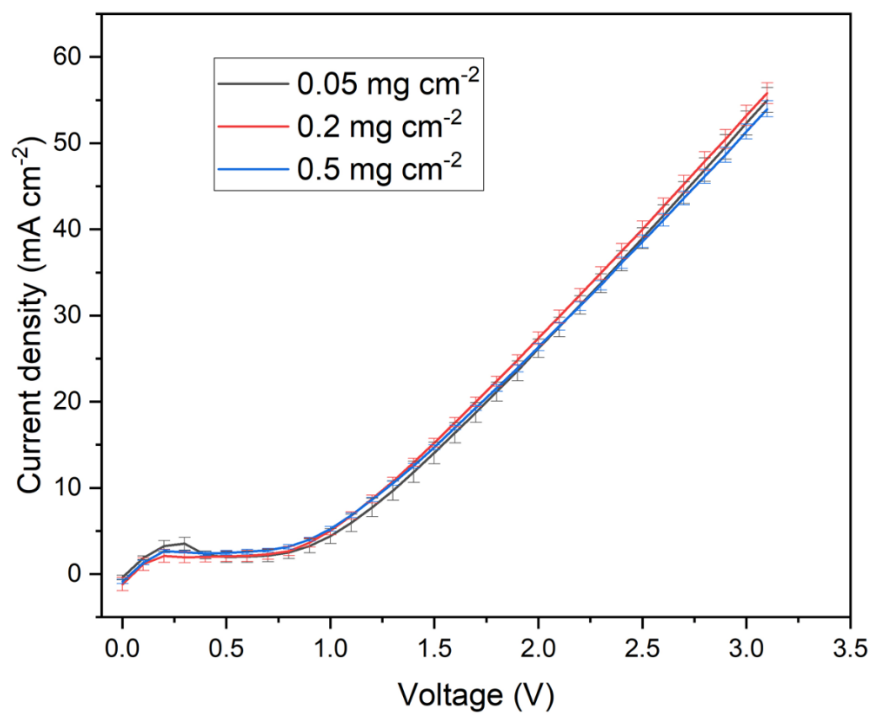


Figure S4. SPEEK/QAPSf polarization behavior with sub-millimeter hole. The limiting current from ionic species crossover cannot be clearly determined.

(a)



(b)

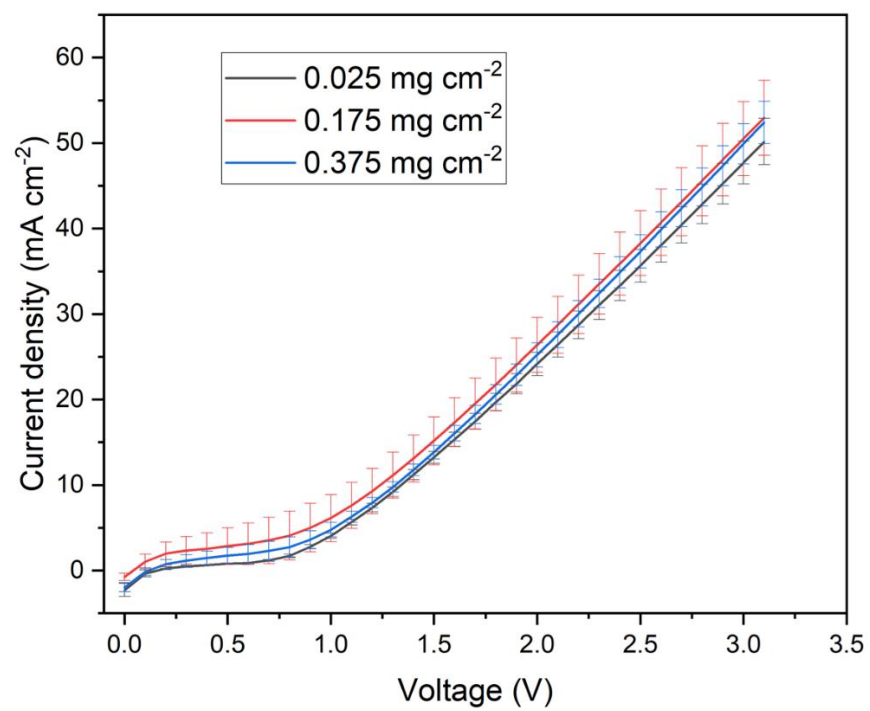


Figure S5. Effect of catalyst loading on (a) flat and (b) patterned SPEEK/QAPSf BPMs.

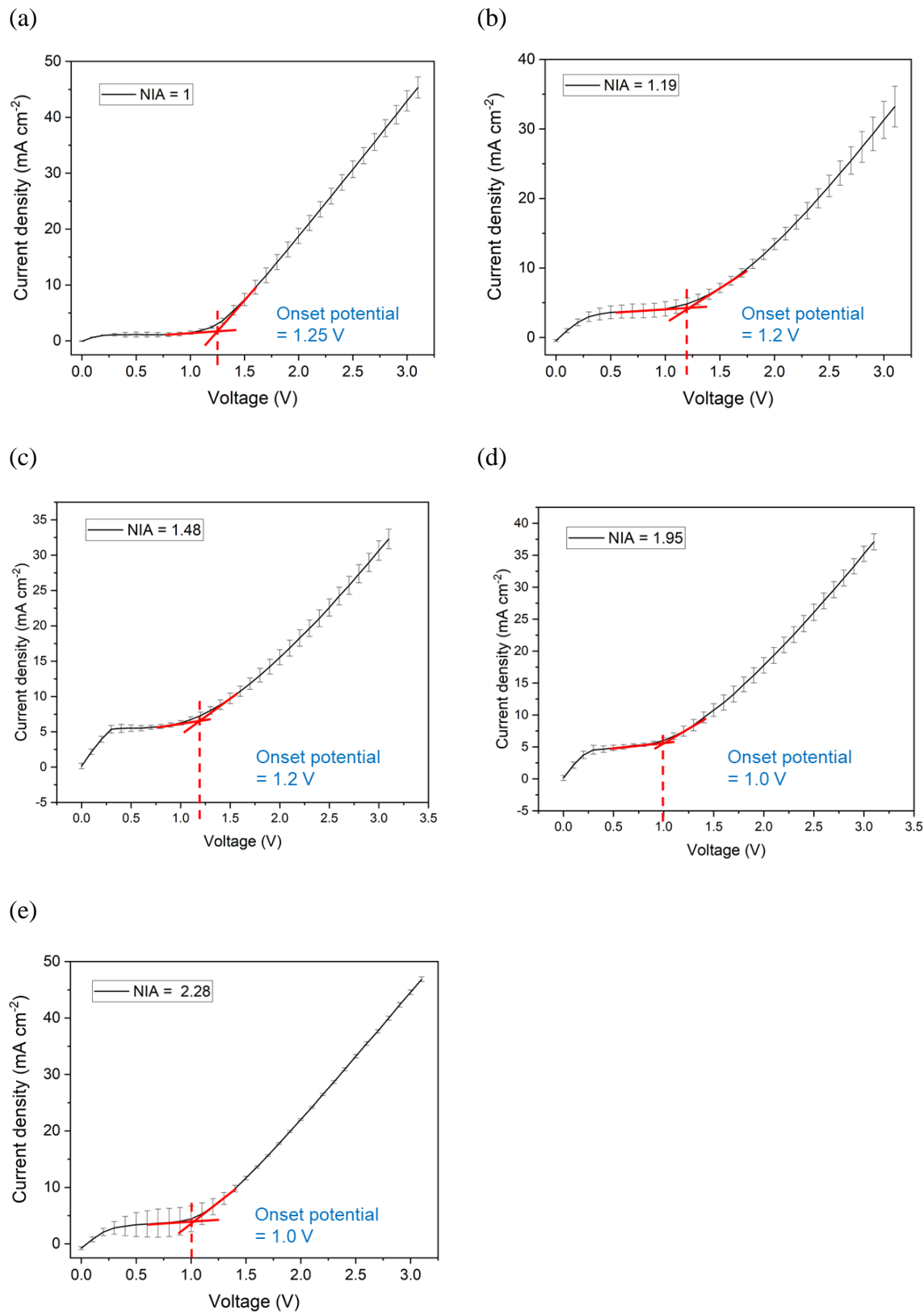


Figure S6. Onset potential for water splitting in SPEEK/QAPSf BPMs of various NIA values.

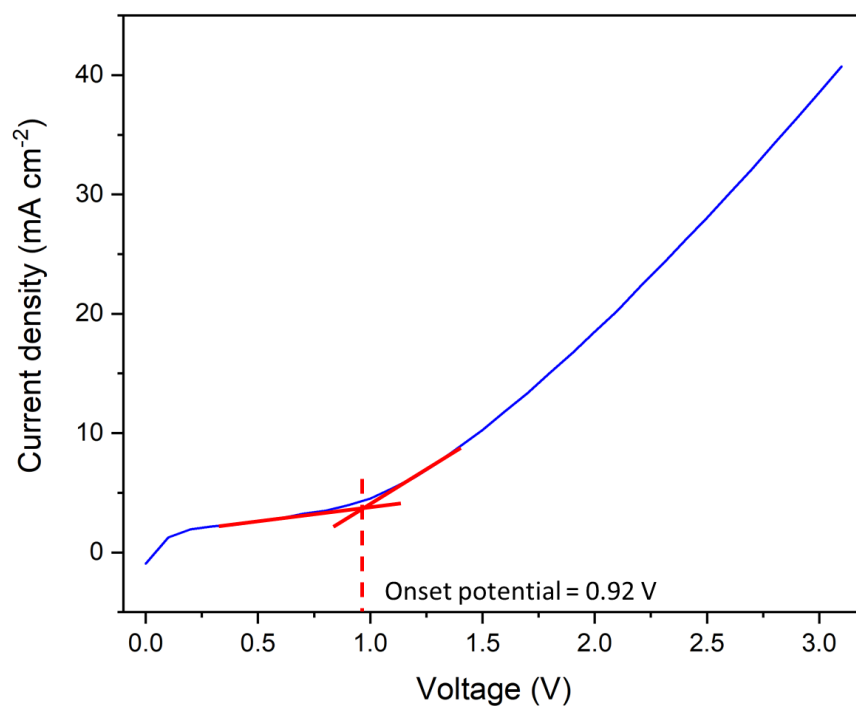


Figure S7. 2-tangent method for determining onset potential for water splitting.

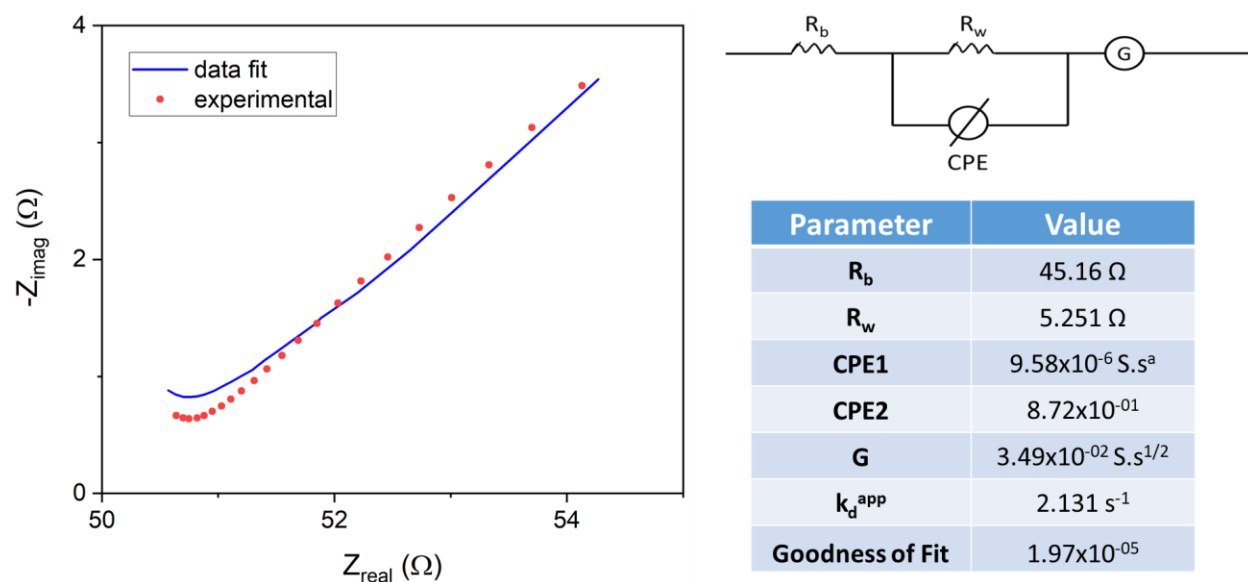


Figure S8. Extraction of k_d^{app} from Gerischer element by data fitting of EIS curve in the low frequency regime of the Nyquist plot.

Density of fixed charges in the bipolar junction (ρ_{BPJ}) was calculated from the average IEC value of AEM and CEM material and density of the membrane material. The calculation for SPEEK/QAPSf BPM is shown below (**equation S1**):

$$\rho_{BPJ} = IEC \cdot \rho \cdot F = 1.65 \frac{mmol}{g} \times 0.001 \frac{mol}{mmol} \times 1.4 \frac{g}{cm^3} \times 96485 \frac{C}{mol} = 2.23 \times 10^2 C cm^{-3} \quad (S1)$$

IEC = Lowest value between the AEM and CEM variant used to make a BPM. 1.65 meq g⁻¹ for SPEEK/QAPSf and SPEEK/Orion BPMs

$$\rho = 1.4 g cm^{-3} \text{ (density of membrane material)}^{[2]}$$

$$F = 96,485 C mol^{-1} \text{ (Faraday's constant)}$$

The local electric field for water splitting at the bipolar junction interface was calculated as shown below for SPEEK/QAPSf BPM (NIA = 1.00) in **equation S2**:

$$E_{loc} = \frac{\rho_{BPJ} \cdot A_{int} \cdot t_{dw}}{\varepsilon} = \frac{\rho_{BPJ} \cdot A_{int} \cdot t_{dw}}{\varepsilon_r \varepsilon_0} = \frac{2.23 \times 10^2 C cm^{-3} \times 1.27 cm^2 \times 20 nm}{40 \times 8.85 \times 10^{-12} C V^{-1} m^{-1}} = 1.6 \times 10^{-8} V m^{-1} \quad (S2)$$

A_{int} = interfacial area of the BPM

t_{dw} = depletion width thickness

ε = permittivity of the hydrated polymer

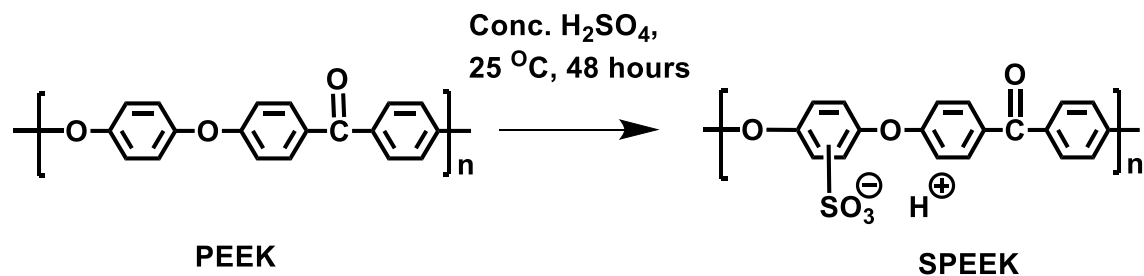
Synthesis of SPEEK

PEEK was dissolved in concentrated H₂SO₄ at room temperature and allowed to react for 2 days. The degree of sulfonation (DS) of PEEK was monitored during the reaction by extracting a solution and precipitating it in copious amounts of DI water to neutralize the sulfuric acid. The precipitated polymer was filtered and dried in a fume hood and then analyzed by ¹H NMR using d₆-DMSO as the solvent. After the desired DS value was obtained, the SPEEK in H₂SO₄ was precipitated using the said procedure. The CEMs from synthesized SPEEK were prepared by dissolving SPEEK into NMP (5 wt%) and then drop casting the solution onto flat glass plates or micropatterned PDMS molds placed on a leveled surface in an oven. The solvent was evaporated from the drop casted SPEEK solution by maintaining the oven temperature at 60 °C for 30 hours.

Synthesis of QAPSF

PSf was dissolved in chloroform to form a 3 wt% solution. Paraformaldehyde and chlorotrimethylsilane were added to the mixture, and the solution was poured into a round bottom flask. The temperature of the flask was raised to 60 °C. Then, the reaction solution was capped with a rubber septum and placed under a nitrogen blanket. Then, the Lewis acid catalyst, SnCl₄, was added. The degree of chloromethylation (DC) was monitored by withdrawing 10 mL of solution from the flask at various time periods. For a given time period, the solution was precipitated in methanol (5:1 volume ratio) followed by filtration. The collected solid was dried and analyzed via ¹H NMR using CDCl₃. Once the desired DC value was achieved, an identical precipitation procedure was followed for the whole solution after cooling the solution to room temperature. The acquired CMPSf solid was redissolved in CHCl₃ (10 wt%) and then reprecipitated in MeOH. In order to prepare AEMs from the resulting polymer, CMPSf was dissolved in NMP to make a 5 wt% solution. N-methyl-pyrrolidine was added to this solution to convert the chloromethylated groups in CMPSf to quaternary ammonium groups. The ionomer solution was then drop casted on to flat glass plates in an oven at 60 °C for 24 hours.

(a)



(b)

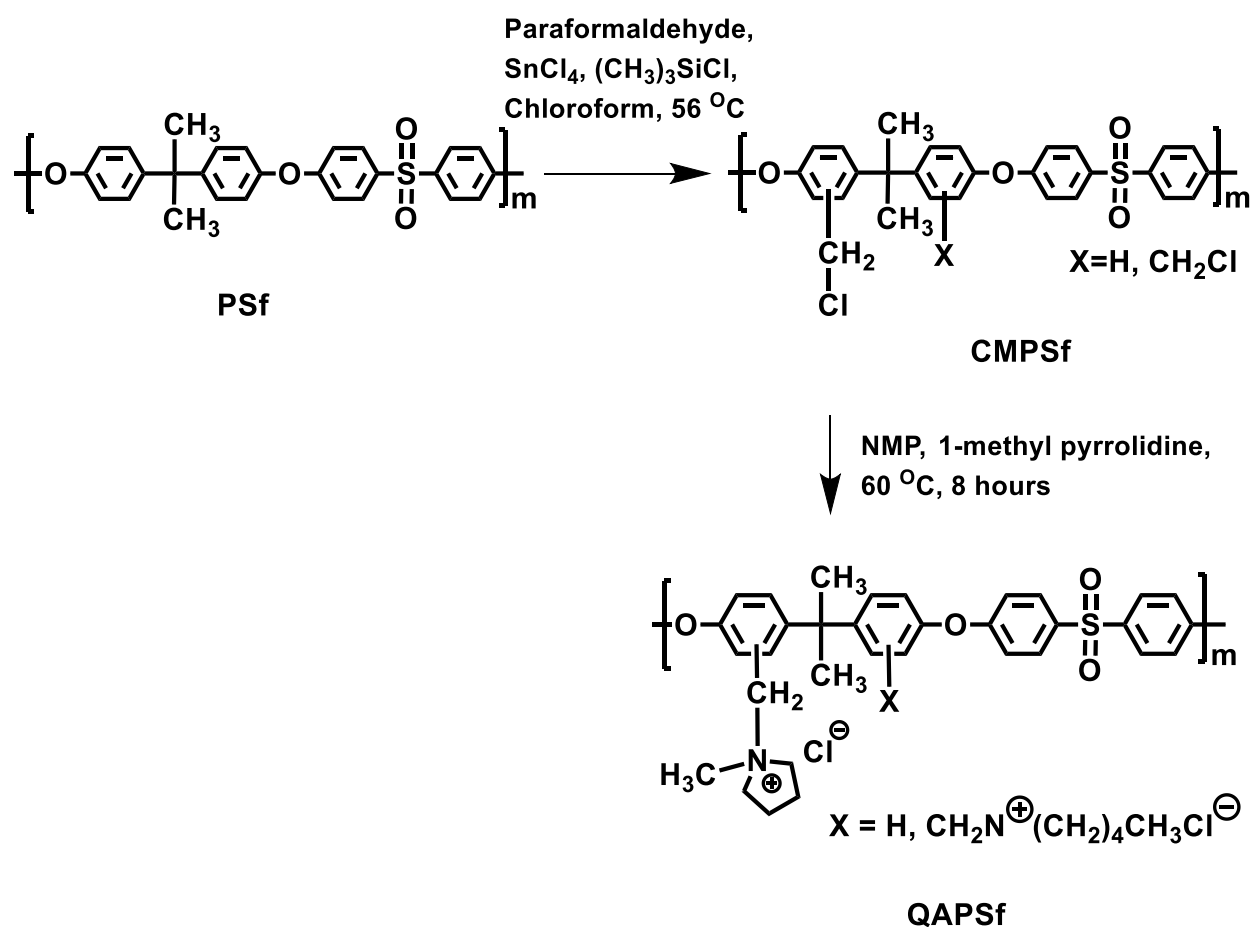
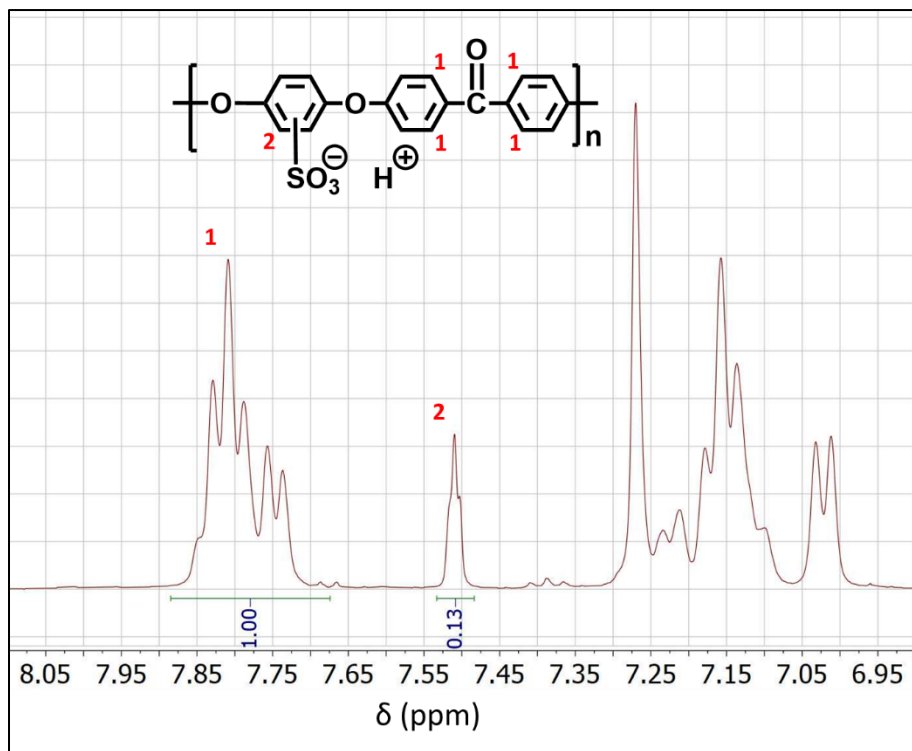
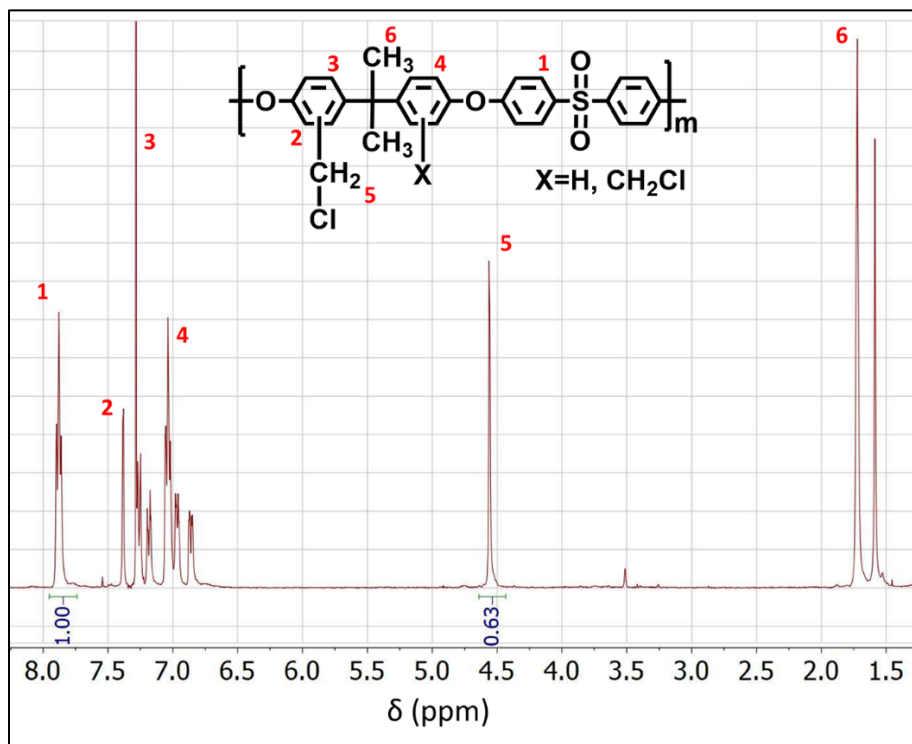


Figure S9. (a) Synthesis scheme for sulfonated poly(arylene ether ether ketone) (SPEEK) by reacting poly(arylene ether ether ketone) (PEEK) with concentrated sulfuric acid followed by neutralization of NaOH solution. (b) Synthesis scheme for QAPSf by i.) chloromethylation of poly(arylene ether) sulfone (PSf) followed by ii.) quaternarization reaction with n-methyl pyrrolidine

(a)



(b)



(c)

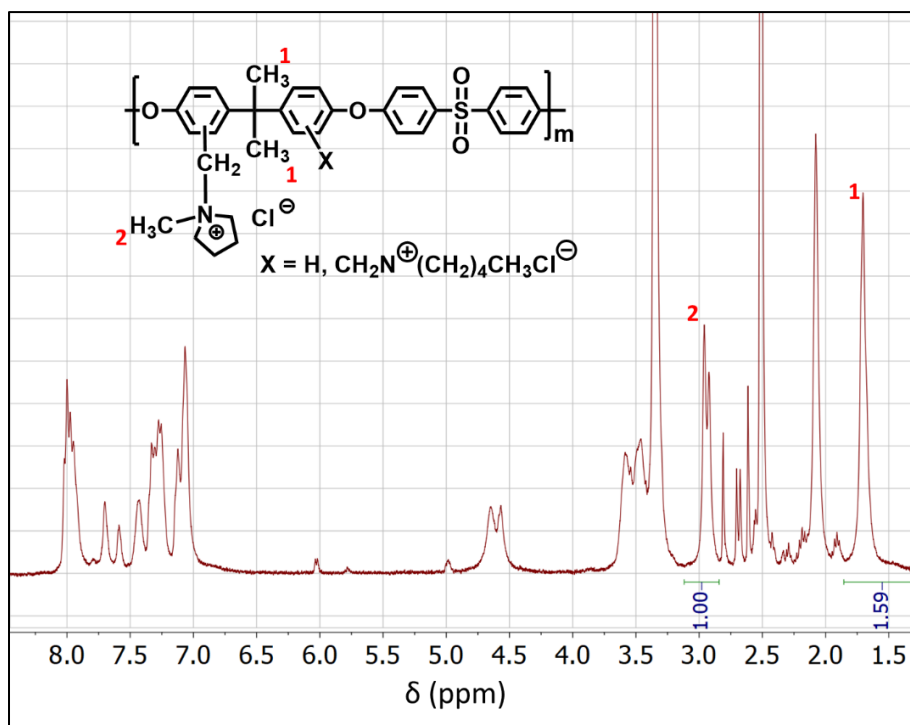


Figure S10. (a) ¹H NMR spectra of SPEEK. The degree of functionalization of sulfonated groups was 0.52 and ion-exchange capacity was 1.65 meq g⁻¹. (b) ¹H NMR spectra of CMPSf. Degree of chloromethylation was 1.26 (c) ¹H NMR spectra of QAPSf. The ion-exchange capacity was 2.34 meq g⁻¹.

The degree of sulfonation (DS) of SPEEK was determined using **equation S3** from the ¹H NMR spectrum of SPEEK in **Figure S11a**. **Equation S4** provides the calculation for SPEEK's IEC from the degree of sulfonation^[3].

$$DS = \frac{4 \text{ Area}(\delta=7.5 \text{ ppm})}{\text{Area}(\delta \approx 7.65 \text{ to } 8.1 \text{ ppm})} \quad (\text{S3})$$

$$\text{IEC} [\text{meq g}^{-1}] = \frac{1000 \text{ DS}}{\text{MW}_{\text{PEEK, monomer}} + \text{DS}(\text{MW}_{\text{SO}_3} + \text{MW}_{\text{H}^+} - 1)} \quad (\text{S4})$$

MW_{PEEK, monomer} = Molecular weight of PEEK repeat unit (g mol⁻¹)

MW_{H^+} = Molecular weight of proton ($g\ mol^{-1}$)

MW_{SO_3} = Molecular weight of SO_3 ($g\ mol^{-1}$)

The degree of chloromethylation (DC) of CMPSf was calculated from its NMR spectrum (**Figure S9b**) and **equation S5**.

$$DC = \frac{2 \cdot \text{Area}(\delta=4.5\ \text{ppm})}{\text{Area}(\delta=7.8\ \text{ppm})} \quad (\text{S5})$$

Conversion of chloromethylated sites to cation sites was calculated from **equation S6** using NMR spectrum of QAPSF in **Figure S11c** and the IEC of QAPSF was calculated^[4] from **equation S7**.

$$\text{Conversion} = \frac{\text{Area}(\delta=2.85\ \text{to}\ 3.15\ \text{ppm})}{2 \cdot DC \cdot \text{Area}(\delta=1.7\ \text{ppm})} \quad (\text{S6})$$

$$IEC[\text{meq}\ g^{-1}] = \frac{1000\ DC}{MW_{\text{PSf, monomer}} + DC(MW_{\text{sodium}} + MW_{\text{chloride}} + MW_{\text{CH}_2 - 1})} \cdot \text{Conversion} \quad (\text{S7})$$

$MW_{\text{PSf, monomer}}$ = Molecular weight of PSf repeat unit ($g\ mol^{-1}$)

MW_{sodium} = Molecular weight of sodium ion ($g\ mol^{-1}$)

MW_{chloride} = Molecular weight of chloride ion ($g\ mol^{-1}$)

MW_{CH_2} = Molecular weight of CH_2 ($g\ mol^{-1}$)

SEM imaging

A FEI Quanta 3D FEG FIB/SEM imaged the surface and cross section of membranes with a backscattered electron detector. The membrane surfaces and cross sections were sputtered with 20 nm of platinum to enhance the imaging contrast. The working distance for imaging ranged from 3 mm to 18 mm. The accelerating voltage for imaging was 5 kV.

Ionic conductivity of AEMs and CEMs

The in-plane ionic conductivity (σ) of AEMs and CEMs were measured with a 4-point platinum probe situated in polytetrafluoroethylene (PTFE) housing. The ionic conductivity measurements were carried out in DI water at room temperature. For measuring AEM hydroxide ion conductivity, the AEMs were ion-exchanged to the hydroxide form using 1 M KOH followed by rinsing with DI water that was bubbled with nitrogen^[5]. The DI water for the conductivity measurement was also treated with nitrogen to minimize carbonation of the AEM^[6]. The in-plane resistance of the membranes was measured via electrochemical impedance spectroscopy (EIS) performed in galvanostatic mode across the frequency range of 100,000 Hz to 0.01 Hz. The alternating current perturbation was 1 mA and ten data points were collected per decade of frequency values. **Equation S8** was used to determine the ionic conductivity of the AEMs and CEMs from the in-plane resistance. **Equation S9** was used to determine the ASR of the AEMs and CEMs. We assume that the AEMs and CEMs have isotropic ion transport. Hence, the in-plane ionic conductivity obtained from **Equation S9** can be used to calculate the through plane-ASR for **Table 1**.

$$\sigma = \frac{d}{L \cdot W \cdot R} \quad (\text{S8})$$

σ = ionic conductivity of the membrane

d = distance between the electrodes where the potential drop is measured

L = membrane thickness

W = width of the membrane thickness in the 4 point probe

R = membrane resistance extracted the Bode plot where the phase angle is equal to 0°

$$ASR = \frac{L}{\sigma} \quad (\text{S9})$$

Permselectivity of AEMs and CEMs

Permselectivity (φ^i) of the AEMs and CEMs was determined from the transference number (T_i) of the membranes. The T_i was calculated from the membranes' junction potential (E) when separating 0.1 M NaCl_{aq} and 0.01 M NaCl_{aq} solutions^[3]. An H-cell partitioned the two liquid cells

with the AEM or CEM. Two Ag/AgCl reference electrodes, one immersed in the compartment containing 0.1 M NaCl_{aq}, and the other in the compartment containing 0.01 M NaCl_{aq}, were used to measure the membrane potential using a multimeter. **Equation S10** relates E to T_i . **Equations S11** and **S12** show how φ^i is calculated from T_i .

$$E = \frac{RT}{zF} \left[T_{counter} \ln \frac{a_{counter}^{conc}}{a_{counter}^{dil}} - T_{co} \ln \frac{a_{co}^{conc}}{a_{co}^{dil}} \right] \quad (\text{S10})$$

$$T_{counter} + T_{co} = 1$$

$T_{counter}$ and T_{co} = the transference number of the corresponding counterion and co-ion for an AEM or CEM

R = Universal gas constant

F = Faraday's constant

z = valence for the ions

a_i = activity coefficients for the counterion or co-ions in the solution. Activity coefficients were calculated using the Debye-Hückel activity coefficient model [3].

$$\varphi^{CEM} = \frac{T_c^{CEM} \cdot T_c}{T_a} \quad (\text{S11})$$

$$\varphi^{AEM} = \frac{T_a^{AEM} \cdot T_a}{T_c} \quad (\text{S12})$$

φ^i = the permselectivity of the AEM or CEM

T_a or T_c = transference number for anion and cation respectively.

Water uptake

Water uptake of the membranes was calculated as a percentage in weight change of the dry membranes before and after immersion in DI water for 24 hours. **Equation S13** was used to calculate the water uptake value. All water uptake measurements were done in sodium ion (CEM) or chloride ion (AEM) form.

$$\text{Water uptake} = \frac{W_2 - W_1}{W_1} \times 100 \% \quad (\text{S13})$$

w_1 = weight of dry membrane

w_2 = weight of membrane after immersion in DI water for 24 hr

Table S2. A summary of bipolar membrane performance from reported values in literature measured by the onset potential for water dissociation and current density at 2V

BPM type (CEM/catalyst/AEM)	Electrolyte type and concentration	Current density @ 2V (mA cm⁻²)	Onset potential (V)
Neosepta CMX/ Fe-MIL-101-NH ₂ / Neosepta AMX ^[7]	0.5 M Na ₂ SO ₄ solution	20	0.3
Sulfonated polyether sulfone (SPES)/ MoS ₂ / IONSEP-HC-A ^[8]	0.4 M NaCl solution	0.8	5.27
Nafion®/GOx/PFAEM (2D BPM) ^[9]	1.0 M NaOH solution (anode)/ 1.0 M H ₂ SO ₄ solution (cathode)	8	4.3
Sulfonated polysulfone/ lysozyme/ quaternized polysulfone ^[10]	0.1 M NaCl solution	25	2.3
SCP commercial CEM/ KFe[Fe(CN) ₆] / SCP commercial AEM ^[11]	2.0 M NaCl solution	6	3
N-methylene phosphonic chitosan/ PEG/ N-methylene phosphonic chitosan ^[12]	0.1 M NaCl solution	12	1
Sulfonated poly(ether ether ketone)/ (Al(OH) ₃)/ Quaternized poly(phenylene oxide) (3D junction BPM) ^[13]	0.5 M Na ₂ SO ₄ solution	375	0.7
Sulfonated poly(ether ether ketone), poly(ether sulfone) blend/ sulfonated poly(ether ether ketone) / aminated polysulfone ^[14]	2.0 M NaCl	15.0	5.0
Nafion™/graphene oxide/ Neosepta AHA AEM ^[15]	1.0 M NaClO ₄	120 (measured at 1.25 V, data not available for 2 V)	0.9
Nafion™/IrO ₂ ,NiO/ Sustainion™-X37-50 ^[16]	1.0 M KOH/ 1.0 M H ₂ SO ₄	300	1.6
Fumasep® BPM ^[13]	0.5 M Na ₂ SO ₄ solution	85 (1.25 V)	0.9

Fumasep [®] BPM ^[17]	1.0M NaOH/ 0.5M H ₂ SO ₄	75 (1.8 V)	1.5
--	---	------------	-----

References

1. Wilhelm FG, Pünt I, van der Vegt NFA, Strathmann H, Wessling M. Asymmetric Bipolar Membranes in Acid–Base Electrodialysis. *Industrial & Engineering Chemistry Research* **2002**, 41:579-586.
2. Mendil-Jakani H, Lopez IZ, Legrand P, Mareau V, Gonon L. A new interpretation of SAXS peaks in sulfonated poly (ether ether ketone)(sPEEK) membranes for fuel cells. *Physical Chemistry Chemical Physics* **2014**, 16:11243-11250.
3. Palakkal VM, Rubio JE, Lin YJ, Arges CG. Low-resistant ion-exchange membranes for energy efficient membrane capacitive deionization. *ACS Sustainable Chemistry & Engineering* **2018**, 6:13778-13786.
4. Arges CG, Parrondo J, Johnson G, Nadhan A, Ramani V. Assessing the influence of different cation chemistries on ionic conductivity and alkaline stability of anion exchange membranes. *Journal of Materials Chemistry* **2012**, 22:3733-3744.
5. Arges C, Wang L, Parrondo J, Ramani V. Best Practices for Investigating Anion Exchange Membrane Suitability for Alkaline Electrochemical Devices: Case Study Using Quaternary Ammonium Poly(2,6-dimethyl 1,4-phenylene)oxide Anion Exchange Membranes. *J. Electrochem. Soc.* **2013**, 160:F1258-F1274.
6. Arges CG, Zhang L. Anion Exchange Membranes' Evolution toward High Hydroxide Ion Conductivity and Alkaline Resiliency. *ACS Applied Energy Materials* **2018**, 1:2991-3012.
7. Wang Q, Wu B, Jiang C, Wang Y, Xu T. Improving the water dissociation efficiency in a bipolar membrane with amino-functionalized MIL-101. *Journal of membrane science* **2017**, 524:370-376.
8. Rathod NH, Sharma J, Raj SK, Yadav V, Rajput A, Kulshrestha V. Fabrication of a Stable and Efficient Bipolar Membrane by Incorporation of Nano-MoS₂ Interfacial Layer for Conversion of Salt into Corresponding Acid and Alkali by Water Dissociation Using Electrodialysis. *ACS Sustainable Chemistry & Engineering* **2020**, 8:13019-13029.
9. Chen Y, Wrubel JA, Klein WE, Kabir S, Smith WA, Neyerlin KC, Deutsch TG. High-Performance Bipolar Membrane Development for Improved Water Dissociation. *ACS Applied Polymer Materials* **2020**.
10. Manohar M, Shukla G, Pandey RP, Shahi VK. Efficient bipolar membrane with protein interfacial layer for optimal water splitting. *Journal of industrial and engineering chemistry* **2017**, 47:141-149.
11. Cheng G, Zhao Y, Li W, Zhang J, Wang X, Dong C. Performance enhancement of bipolar membranes modified by Fe complex catalyst. *Journal of Membrane Science* **2019**, 589:117243.
12. Rajesh AM, Kumar M, Shahi VK. Functionalized biopolymer based bipolar membrane with poly ethylene glycol interfacial layer for improved water splitting. *Journal of membrane science* **2011**, 372:249-257.
13. Shen C, Wycisk R, Pintauro PN. High performance electrospun bipolar membrane with a 3D junction. *Energy & Environmental Science* **2017**, 10:1435-1442.
14. Balster J, Srinantharajah S, Sumbharaju R, Pünt I, Lammertink RG, Stamatialis D, Wessling M. Tailoring the interface layer of the bipolar membrane. *Journal of membrane science* **2010**, 365:389-398.
15. McDonald MB, Freund MS. Graphene Oxide as a Water Dissociation Catalyst in the Bipolar Membrane Interfacial Layer. *ACS Applied Materials & Interfaces* **2014**, 6:13790-13797.

16. Oener SZ, Foster MJ, & Boettcher SW. Accelerating water dissociation in bipolar membranes and for electrocatalysis. *Science* **2020**, 369(6507), 1099-1103.
17. Xu J, Amorim I, Li Y, Li J, Yu Z, Zhang B, Araujo A, Zhang N, Liu L. Stable overall water splitting in an asymmetric acid/alkaline electrolyzer comprising a bipolar membrane sandwiched by bifunctional cobalt-nickel phosphide nanowire electrodes. *Carbon Energy* **2020**, 2(4), 646-655.